Article

Quantum-enhanced nonlinear microscopy

https://doi.org/10.1038/s41586-021-03528-w

Received: 31 March 2020

Accepted: 9 April 2021

Published online: 9 June 2021

Check for updates

Catxere A. Casacio[1], Lars S. Madsen[1], Alex Terrasson[1], Muhammad Waleed[1], Kai Barnscheidt[2], Boris Hage[2], Michael A. Taylor[3] & Warwick P. Bowen[1]✉

The performance of light microscopes is limited by the stochastic nature of light, which exists in discrete packets of energy known as photons. Randomness in the times that photons are detected introduces shot noise, which fundamentally constrains sensitivity, resolution and speed[1]. Although the long-established solution to this problem is to increase the intensity of the illumination light, this is not always possible when investigating living systems, because bright lasers can severely disturb biological processes[2–4]. Theory predicts that biological imaging may be improved without increasing light intensity by using quantum photon correlations[1,5]. Here we experimentally show that quantum correlations allow a signal-to-noise ratio beyond the photodamage limit of conventional microscopy. Our microscope is a coherent Raman microscope that offers subwavelength resolution and incorporates bright quantum correlated illumination. The correlations allow imaging of molecular bonds within a cell with a 35 per cent improved signal-to-noise ratio compared with conventional microscopy, corresponding to a 14 per cent improvement in concentration sensitivity. This enables the observation of biological structures that would not otherwise be resolved. Coherent Raman microscopes allow highly selective biomolecular fingerprinting in unlabelled specimens[6,7], but photodamage is a major roadblock for many applications[8,9]. By showing that the photodamage limit can be overcome, our work will enable order-of-magnitude improvements in the signal-to-noise ratio and the imaging speed.

Light microscopy is a powerful tool to understand the microscopic structure and dynamics of living systems. Recent advances range from super-resolution microscopes that allow the imaging of biomolecules at near-atomic resolution[10], to light-sheet techniques that rapidly explore living cells in three dimensions[11] and high-speed microscopes for optogenetic control of neural networks[12]. The sensitivity, resolution and speed of these microscopes is fundamentally limited by shot noise, which arises because light is quantized into photons[1]. The effects of shot noise can be reduced by increasing the intensity of the illumination light. However, for many advanced microscopes, this approach is no longer tenable due to the intrusion of the light on biological processes[2,9,13]. Light is known to disturb function, structure and growth[3,9,13], and is ultimately fatal[3,9].

It has been known for many decades that quantum correlations can be used to extract more information per photon used in an optical measurement[5]. This allows the trade-off between the signal-to-noise ratio and intensity to be broken[14]. Indeed, for this reason, quantum correlations are now used routinely to improve the performance of laser interferometric gravitational wave detectors[15]. They have also been shown to improve many other optical measurements in proof-of-principle experiments[16]. The importance of improving sensitivity has motivated efforts to apply quantum-correlated illumination to microscopy[1,17], with recent demonstrations of quantum-enhanced absorption[18–22] and phase-contrast[23–25] imaging. Quantum correlations have also been used for illumination in infrared spectroscopic imaging[26] and optical coherence tomography[27]. However, all previous experiments used optical intensities more than 12 orders of magnitude lower than those for which biophysical damage typically arises[4], and far below the intensities typically used in precision microscopes. They therefore did not provide an absolute sensitivity advantage—superior sensitivity could have been achieved in the absence of quantum correlations using higher optical power. Increasing the illumination intensity to levels relevant for high-performance microscopy is a longstanding challenge that has proved difficult owing to limitations in the methods used to produce quantum correlations, to their fragility once produced and to the challenge of integration within a precision microscope.

Here we develop a coherent Raman scattering microscope that incorporates bright quantum-correlated illumination. Coherent Raman microscopes are a form of nonlinear microscope that probe the vibrational spectra of biomolecules[6,8]. They allow unlabelled imaging of chemical bonds with exceptionally high specificity—far higher than is possible, for example, using fluorescence[6,7]. This provides new capabilities to study a wide range of biological processes, including metabolic processes[28], nerve degeneration[29], neuron membrane potentials[30] and antibiotic response[31]. However, photodamage places acute constraints on sensitivity and imaging speed[6,8,9], presenting a roadblock for powerful prospective applications such as label-free spectrally multiplexed imaging[7]. State-of-the-art coherent Raman microscopes are already limited by shot noise[32,33]. Consequently, the roadblock cannot be overcome through improvements in instrumentation.

The quantum correlations in our coherent Raman microscope allow the shot-noise limit to be broken, providing the possibility of

[1]ARC Centre of Excellence for Engineered Quantum Systems, University of Queensland, St Lucia, Queensland, Australia. [2]Institut für Physik, Universität Rostock, Rostock, Germany. [3]Australian Institute for Bioengineering and Nanotechnology, The University of Queensland, St Lucia, Queensland, Australia. ✉e-mail: w.bowen@uq.edu.au

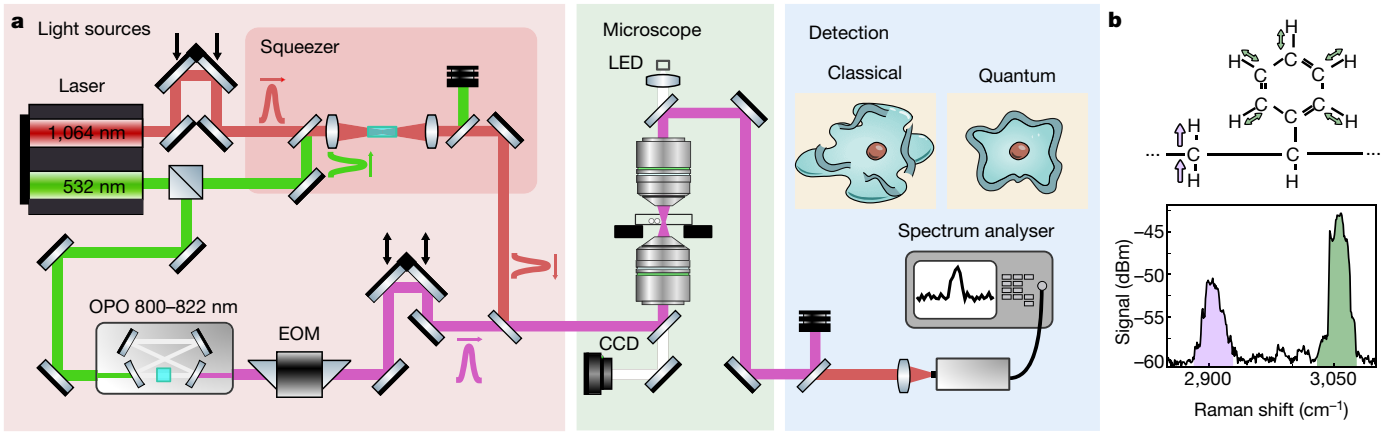

Fig. 1 | Experimental setup. a, Setup schematics. Left, preparation of the pump beam (purple) via an optical parametric oscillator (OPO) and 20-MHz modulation from an electro-optic modulator (EOM), and of the Stokes beam (red) that is amplitude-squeezed in a periodically poled $KTiOPO_4$ crystal pumped with 532-nm light. Middle, stimulated Raman scattering is generated in samples at the microscope focus, with raster imaging performed by scanning the sample through the focus. A charge-coupled device (CCD) camera and a light-emitting diode (LED) allow simultaneous bright-field microscopy. Right, after filtering out the pump, the Stokes beam is detected and the signal processed using a spectrum analyser. For all experiments, 3 mW of detected Stokes power was used. **b**, Raman spectra measured from a 3-μm polystyrene bead, showing the CH_2 antisymmetric stretch (purple) and CH aromatic stretch (green) resonances. Spectra taken with 100-kHz spectrum analyser resolution bandwidth (RBW).

an improved signal-to-noise ratio, sensitivity and imaging speed. When imaging the interior of a cell, we show that they enhance the signal-to-noise ratio by 35%. Combined with subwavelength resolution and few-millimolar-per-root-hertz concentration sensitivity, this allows biological features to be seen that would have otherwise been buried beneath the shot noise. Light-induced damage is directly observed. This imposes a hard bound on intensity, limiting the maximum possible signal-to-noise ratio when using coherent illumination. Our microscope operates safely beyond this limit, showing that quantum correlations can evade light-induced damage. This removes a fundamental barrier to advances in coherent Raman microscopy and high-performance microscopy more broadly.

Quantum-compatible nonlinear microscope

In Raman scattering, a pump photon inelastically scatters from a molecule, exciting a chemical bond vibration and re-emitting a lower-frequency Stokes photon. The frequency shift, or Raman shift, between pump and Stokes photons corresponds to the vibrational frequency of the bond, providing spectroscopic information about the molecule. However, Raman scattering is inherently weak[7,8]. Coherent Raman microscopes enhance the process using resonant driving from multiple lasers[8]. The particular microscope we construct is a custom-designed stimulated Raman microscope (Fig. 1a, details in Supplementary Information sections 1–5) that uses excitation lasers at both pump and Stokes frequencies[6]. The rate of stimulated Raman scattering, and hence the signal-to-noise ratio, depends on the product of pump and Stokes laser intensities. Consequently, we combine high-numerical-aperture objectives with picosecond-pulsed lasers to reach high peak intensities. To avoid degradation of quantum correlations, the objectives are custom-built to each have Stokes transmission >92%. At the output of the microscope, the Stokes light is detected on a custom-designed photodetector with very low electronic noise and high bandwidth. Together with previously established laser noise minimization techniques that shift the Raman signal into modulation sidebands around the Stokes frequency[34], this allows shot-noise-limited operation with relative intensity noise comparable to state-of-the-art stimulated Raman microscopes[32,34].

Before introducing quantum correlations, we systematically explore the Raman signal strength using dry monodisperse samples of polystyrene beads. Figure 1b shows a typical Raman spectrum, exhibiting several Raman bands. We focus here on the CH aromatic stretch band, monitoring its Raman signal as the pump power is gradually increased over time. At low pump powers, the signal strength rises as expected with intensity. However, at high powers it diverges, typically decreasing markedly and decaying over time, as shown for example in Fig. 2a. This is a signature of the onset of photodamage (Fig. 2a, Supplementary Information section 6). To determine the statistics of the power at which this onset occurs, we repeat the measurement on 110 beads. The resulting histogram and cumulative probability distribution are shown in Fig. 2b, c.

Quantum correlations suppress noise

To increase the signal-to-noise ratio of the microscope, we introduce quantum correlations between Stokes photons using a purpose-built optical parametric amplifier (Supplementary Information sections 7–10). The correlations suppress, or 'squeeze', the amplitude noise on the Stokes field at the frequency of the stimulated Raman modulation sidebands (Fig. 3a, dashed line), while leaving the Raman signal strength unchanged (though spatiotemporal modeshape changes can affect this, Supplementary Information section 8.3). Similar quantum correlations—albeit in continuous-wave light fields with far lower peak intensity—have been applied in several biophysically relevant proof-of-principle experiments, demonstrating improvements in sensitivity[35–37], resolution[23,38,39] and fundamental capabilities[26,27,40]. Used here they allow Raman scattering to be observed even when less than one photon is scattered on average during the measurement interval, removing what is otherwise a strict constraint on the photon budget[8,13]. Figure 3b shows the power spectrum of the Raman photocurrent when using quantum-squeezed Stokes light, again probing the CH aromatic stretch band of a 3-μm polystyrene bead. The peak in the spectrum is the stimulated Raman signal. Quantum correlations reduce the noise floor by a factor of 13% (−0.6 dB) beneath the usual shot-noise limit, consistent with expectations given the inefficiencies of our apparatus (Supplementary Information section 10).

The signal-to-noise ratio is defined as the ratio of the height of the stimulated Raman peak to the power spectrum noise floor. We find that it initially increases quadratically with Raman pump power, as expected for stimulated Raman scattering[34]. However, as shown

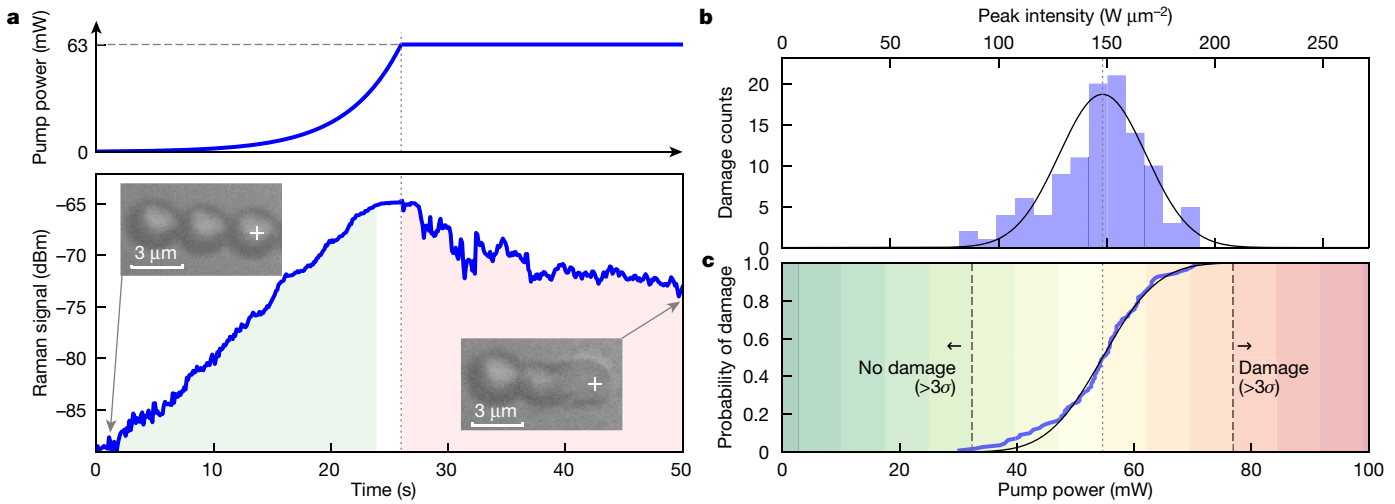

Fig. 2 | Quantifying photodamage. Raman signal from the CH aromatic stretch band of a 3-µm polystyrene bead as a function of pump power with a fixed 3-mW Stokes power. **a**, Top, the pump power is gradually increased until photodamage is observed, in this example occurring at a power at the sample of 63 mW. It is then held fixed. Bottom, the Raman signal increases with power before photodamage (green) and drops at fixed pump intensity after the particle is damaged (red). Visual inspection (insets) confirms that photodamage has occurred. RBW, 1 kHz. Cross-hairs, position of laser focus. **b**, **c**, Characterization of the photodamage threshold for 110 particles. **b**, Histogram of the pump power at which the observed Raman signal visibly diverges from damage-free expectations. The Gaussian fit yields a mean photodamage threshold of 54.6 mW (dashed line; intensity, 150 W µm^{-2}) and a standard deviation of 7.4 mW. **c**, Corresponding cumulative distribution, with the dotted line indicating the mean and each shaded bar corresponding to +1σ from the mean.

for one example in Fig. 3c, the manifestation of photodamage prevents this scaling from continuing indefinitely. When using shot-noise-limited light, there is a strict maximum in the damage-free signal-to-noise ratio, which for the example of Fig. 3c has mean ± s.d. of $SNR_{max}^{shot\ noise} = 88.2 \pm 0.2$ from a measurement with 3-kHz-resolution bandwidth. Quantum correlations provide a damage-free signal-to-noise ratio of $SNR_{max}^{quantum} = 99.2 \pm 0.3$, corresponding to an enhancement of $SNR_{max}^{quantum}/SNR_{max}^{shot\ noise} - 1 = 12.5 \pm 0.4\%$. This represents an absolute quantum advantage—with the same spatiotemporal modes and apparatus, photodamage prohibits classical techniques from reaching this level of signal-to-noise ratio. It contrasts with previous demonstrations of quantum-illumination-enhanced imaging[18–25], where equivalent performance could be attained by increasing the classical illumination intensity.

The concentration sensitivity of a Raman microscope can be directly calculated from its signal-to-noise ratio. After improvements in alignment made for cell imaging (discussed below), we find a concentration sensitivity for the styrene monomers that form polystyrene of 7.8 mM for a 1-s integration period, enhanced by 7% due to quantum correlations (Supplementary Information section 11). Although a much better concentration sensitivity is possible for other bonds[6], this is comparable to previous high-sensitivity stimulated Raman measurements of the CH aromatic stretch band of polystyrene[41] (Supplementary Information section 11).

We note two parallel demonstrations of quantum-enhanced nonlinear spectroscopy[42,43]. Both use peak optical intensities well below the levels used in state-of-the-art nonlinear microscopes and do not observe photodamage. Nor do they perform imaging, although ref. [42] does report spatially distributed measurements. Our combination of pulsed excitation and high-numerical-aperture objectives enables orders-of-magnitude higher peak intensities for both pump and Stokes fields. This brings the microscope into the regime where photodamage is relevant, and increases the nonlinear signal amplitude (proportional to the product of peak intensities) by around a factor of 10^8.

Quantum-enhanced imaging

To demonstrate quantum-enhanced imaging, we record the power of the stimulated Raman signal as the microscope sample stage is raster-scanned over samples of both dry polystyrene beads and living *Saccharomyces cerevisiae* yeast cells in aqueous solution (details in Supplementary Information section 12). A pixel dwell time of 50 ms is used, limited by our stage scanning system. This is comparable to dwell times used in previous Raman imaging of yeast cells[44,45], but is relatively long compared with state-of-the-art video-rate imaging[32]. The 40-MHz bandwidth of quantum enhancement demonstrated (Fig. 3a) is compatible with the faster scanning systems necessary for video-rate imaging, indicating that quantum-enhanced video-rate imaging should be possible in future.

Figure 4a shows a typical quantum-enhanced image of a collection of 3-µm polystyrene beads, with a signal-to-noise ratio enhanced by 23% compared with the shot-noise limit. Figure 4b shows the equivalent image for a single yeast cell, in this case recorded at a Raman shift of 2,850 cm^{-1} to target the CH_2 bonds that are most prevalent in lipids. Improved alignment of the microscope and squeezed light source, together with lower Fresnel reflective losses at water–glass interfaces compared with air, in this case allow a 35% enhancement in the signal-to-noise ratio, increasing the contrast of the image (see direct comparison in Supplementary Information section 12.3). This corresponds to a 14% improvement in concentration sensitivity. Visible cell damage was observed at higher pump intensities (Fig. 4c). Without quantum correlations or exposing the sample to these higher intensities, a 35% higher pixel dwell time would be required to achieve the same contrast (Supplementary Information section 13), which would reduce the frame rate of the microscope and increase the photochemical formation of damaging hydroxyl radicals[9]. The enhanced contrast is particularly useful in subcellular imaging as many features have far-subwavelength dimensions and produce correspondingly small Raman signals.

When imaging yeast cells, the microscope benefits fully from the use of high-numerical-aperture water-immersion objectives that, together with the nonlinearity of the Raman interaction, enable subwavelength resolution (Fig. 4b). Compared with the bright-field microscope image in the inset of Fig. 4b, the stimulated Raman image provides much more information about the interior cell structure. The Raman signal from cytosol is visible across the entire cell volume, together with five bright organelles that have a size and

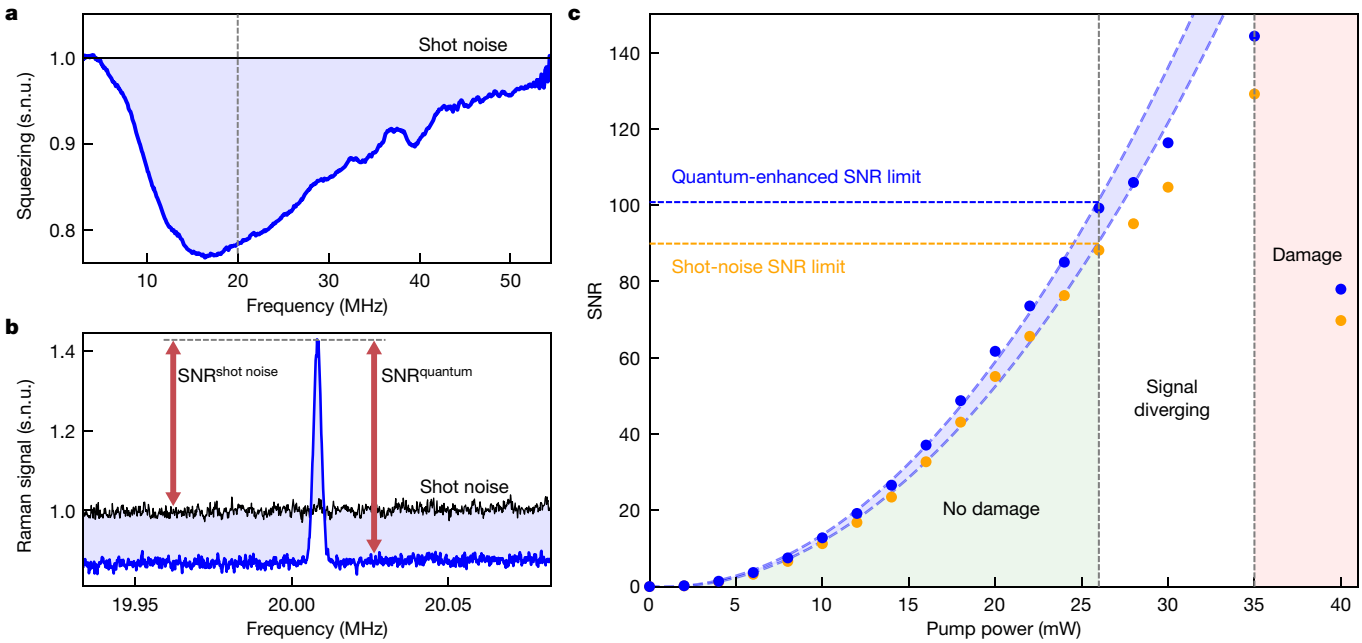

Fig. 3 | Quantum-enhanced stimulated Raman microscopy. a, Noise spectrum of squeezed light normalized to shot noise (s.n.u., shot-noise units). The maximum squeezing of 22% (or −1.1 dB) is achieved near the 20-MHz Raman modulation frequency (vertical dashed line). RBW, 1 MHz. **b**, Stimulated Raman signal of a 3-μm polystyrene bead using 3 mW of pump light at the sample. Squeezed Stokes light reduces the total measurement noise to 13% below the shot noise (or −0.60 dB), improving the signal-to-noise ratio (SNR) by 15%. **c**, Signal-to-noise ratio for one 3-μm polystyrene particle with increasing pump power. The quantum-enhanced signal-to-noise ratio is determined directly, with the shot-noise-limited signal-to-noise ratio inferred from the ratio of shot-noise-limited and quantum-enhanced noise floors. This ensures a fair comparison, insensitive to spatiotemporal modeshape variations between the measurements (Supplementary Information section 8.3). The statistically determined 1σ uncertainty for all signal-to-noise ratios is less than 1%. The signal-to-noise ratio increases quadratically as expected until 26 mW (green), indicating that the particle is undamaged. The common fluctuations of the shot-noise-limited and squeezed signal-to-noise ratios about this quadratic dependence are consistent with 1%-level laser intensity drift. Above 26 mW, the signal-to-noise ratio rises more slowly (white), suggestive of some disruption within the particle, and finally drops (red) when the power reaches the threshold for visible damage. Dashed lines, fits to undamaged signal-to-noise ratio; blue shading, quantum enhancement. RBW, 3 kHz (**b**, **c**); video bandwidth, 10 Hz (**a**–**c**).

composition consistent with lipid droplets[45] (Supplementary Information section 12.1). The signal-to-noise ratio of the cytosol signal is approximately 3, and would reduce to 2 using shot-noise-limited illumination. The peak signal-to-noise ratio from the lipid droplets is around 100. As such, the pixel dwell time of the microscope could be reduced to around 500 μs before the Raman signal from the cell became fully unresolved. Without quantum correlations, this would occur at the longer dwell time of 680 μs. A thin semicircular feature consistent with a section of the cell membrane or wall is also resolved in Fig. 4b. Raman signals from these structures are typically faint due to their tens-of-nanometres thickness. Here quantum correlations allow an approximately 40% longer length of the feature to be resolved than would have been possible with coherent illumination (Supplementary Information section 12.3).

Discussion and outlook

By reporting a nonlinear microscope with quantum-enhanced sensitivity and using it to improve cell imaging, our work demonstrates the long-recognized potential of quantum-correlated illumination to overcome performance barriers in microscopy[5]. Our implementation within a coherent Raman microscope provides the capacity for wide impact due to the extremely high specificity and label-free operation such microscopes provide. Coherent Raman microscopes have seen broad applications over the past decade[6,8], but their speed and sensitivity have been constrained by optical shot noise[32,33]. Faster and more sensitive imaging currently requires alternative methods such as fluorescence imaging, for which labels provide far higher cross-sections than are available in label-free Raman scattering. By overcoming the shot-noise limit, our work opens a pathway towards important applications, such as video-rate imaging of weak molecular vibrations and label-free spectrally resolved imaging[6,7]. Our work shows that sensors that use quantum correlations can achieve signal-to-noise ratios beyond the photodamage-free capacity of conventional techniques. Photodamage-evading microscopes of the kind demonstrated here are broadly recognized as a key metrological application of quantum technologies[46], providing a path to exceed severe constraints on existing high-performance microscopes that would otherwise be fundamental[2,13].

In absolute terms, the level of improvement achieved here is relatively low. This is due, in large part, to the relative immaturity of technology capable of generating and detecting bright picosecond squeezed light, together with the relatively low total optical efficiency for squeezed light in our apparatus of approximately 40%. Although it may be challenging to achieve high collection efficiency in vivo[32], absorption and scattering of in vitro samples is typically very low, as evidenced by the poor contrast of simple bright-field imaging, and therefore should not present a substantial constraint. Continuous-wave squeezing technology that provides as much as a factor of 30 enhancement in the signal-to-noise ratio has been developed to improve the capabilities of gravitational wave detectors[47]. Even allowing for additional optical loss from two high-numerical-aperture objectives, this suggests that an order-of-magnitude improvement in the damage-free signal-to-noise ratio is feasible in future quantum-enhanced coherent Raman microscopes, or equivalently that their frame rate could be increased by the same margin without reducing the signal-to-noise ratio. Such an improvement would otherwise only be possible using contrast agents with large Raman

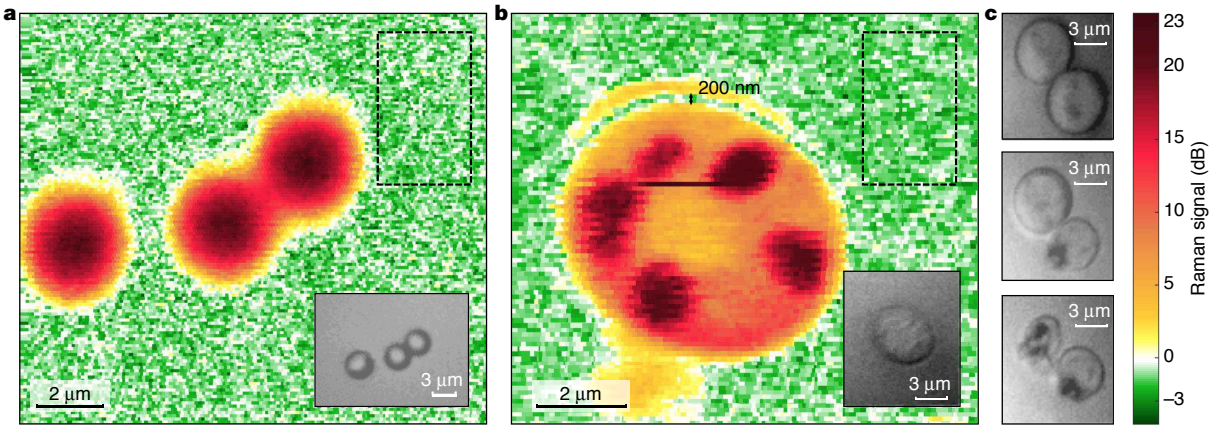

Fig. 4 | Quantum-enhanced imaging. a, Image of 3-µm polystyrene beads at a Raman shift of 3,055 cm^{-1} obtained with 6 mW of pump power at the sample. The background (coloured green) has no Raman signal, and is limited by measurement noise, which is 0.9 dB below shot noise, providing a 23% increase in the signal-to-noise ratio. **b**, Image of a live yeast cell (*Saccharomyces cerevisiae*) in aqueous buffer at 2,850 cm^{-1} Raman shift. Several organelles are clearly visible. The faint outline of what may be the cell membrane or wall is also visible, showing that the microscope has a resolution of around 200 nm. Here the measurement noise is reduced by 1.3 dB below shot noise, corresponding to a 35% signal-to-noise ratio improvement. This image was recorded with around 30 mW of pump power at the sample. The pump intensity of 210 W $µm^{-2}$ was beneath that at which visible cell damage was observed. Dashed rectangular boxes in **a**, **b** show the regions used to determine the measurement noise and the insets are bright-field microscopy images. RBW, 1 kHz; video bandwidth, 10 Hz. **c**, A sequence of images in which two cells are illuminated with the same pump power as in **b** but focused to roughly a factor of two higher intensity. Visible photodamage is observed after only a few seconds of exposure (middle and bottom images).

scattering cross-sections[7], forgoing label-free operation. Quantum correlations could also be used to operate with lower light intensities and thereby suppress performance-limiting noise processes such as out-of-focus fluorescence and background scatter[48], to improve the single-molecule imaging sensitivity of plasmon-enhanced Raman microscopes[49] or even to enhance the cross-section of Raman scattering and therefore signal strength[50].

Online content

Any methods, additional references, Nature Research reporting summaries, source data, extended data, supplementary information, acknowledgements, peer review information; details of author contributions and competing interests; and statements of data and code availability are available at https://doi.org/10.1038/s41586-021-03528-w.

1. Taylor, M. A. & Bowen, W. P. Quantum metrology and its application in biology. *Phys. Rep.* **615**, 1–59 (2016).
2. Li, B., Wu, C., Wang, M., Charan, K. & Xu, C, An adaptive excitation source for high-speed multiphoton microscopy. *Nat. Methods* **17**, 163–166 (2020).
3. Wäldchen, S., Lehmann, J., Klein, T., Van De Linde, S. & Sauer, M. Light-induced cell damage in live-cell super-resolution microscopy. *Sci. Rep.* **5**, 15348 (2015).
4. Mauranyapin, N. P., Madsen, L. S., Taylor, M. A., Waleed, M. & Bowen, W. P. Evanescent single-molecule biosensing with quantum-limited precision. *Nat. Photon.* **11**, 477–481 (2017).
5. Slusher, R. E. Quantum optics in the '80s. *Opt. Photon. News* **1**, 27–30 (1990).
6. Cheng, J.-X. & Sunney Xie, X. Vibrational spectroscopic imaging of living systems: an emerging platform for biology and medicine. *Science* **350**, aaa8870 (2015).
7. Wei, L. et al. Super-multiplex vibrational imaging. *Nature* **544**, 465–470 (2017).
8. Camp, C. H. Jr & Cicerone, M. T. Chemically sensitive bioimaging with coherent Raman scattering. *Nat. Photon.* **9**, 295–305 (2015).
9. Fu, Y., Wang, H., Shi, R. & Cheng, J.-X. Characterization of photodamage in coherent anti-Stokes Raman scattering microscopy. *Opt. Express* **14**, 3942–3951 (2006).
10. Sigal, Y. M., Zhou, R. & Zhuang, X. Visualizing and discovering cellular structures with super-resolution microscopy. *Science* **361**, 880–887 (2018).
11. Alex, M. et al. Applying systems-level spectral imaging and analysis to reveal the organelle interactome. *Nature* **546**, 162–167 (2017).
12. Adam, Y. et al. Voltage imaging and optogenetics reveal behaviour-dependent changes in hippocampal dynamics. *Nature* **569**, 413–417 (2019).
13. Schermelleh, L. et al. Super-resolution microscopy demystified. *Nat. Cell Biol.* **21**, 72–84 (2019).
14. Sewell, R. J., Napolitano, M., Behbood, N., Colangelo, G. & Mitchell, M. W. Certified quantum non-demolition measurement of a macroscopic material system. *Nat. Photon.* **7**, 517–520 (2013).
15. Aasi, J. et al. Enhanced sensitivity of the LIGO gravitational wave detector by using squeezed states of light. *Nat. Photon.* **7**, 613–619 (2013).
16. Giovannetti, V., Lloyd, S. & Maccone, L. Advances in quantum metrology. *Nat. Photon.* **5**, 222–229 (2011).
17. Moreau, P.-A., Toninelli, E., Gregory, T. & Padgett, M. J. Imaging with quantum states of light. *Nat. Rev. Phys.* **1**, 367–380 (2019).
18. Brida, G., Genovese, M. & Ruo Berchera, I. Experimental realization of sub-shot-noise quantum imaging. *Nat. Photon.* **4**, 227–230 (2010).
19. Defienne, H., Reichert, M., Fleischer, J. W. & Faccio, D. Quantum image distillation. *Sci. Adv.* **5**, eaax0307 (2019).
20. Sabines-Chesterking, J. et al. Twin-beam sub-shot-noise raster-scanning microscope. *Opt. Express* **27**, 30810–30818 (2019).
21. Samantaray, N., Ruo-Berchera, I., Meda, A. & Genovese, M. Realization of the first sub-shot-noise wide field microscope. *Light Sci. Appl.* **6**, e17005 (2017).
22. Gregory, T., Moreau, P.-A., Toninelli, E. & Padgett, M. J. Imaging through noise with quantum illumination. *Sci. Adv.* **6**, eaay2652 (2020).
23. Israel, Y., Rosen, S. & Silberberg, Y. Supersensitive polarization microscopy using NOON states of light. *Phys. Rev. Lett.* **112**, 103604 (2014).
24. Ono, T., Okamoto, R. & Takeuchi, S. An entanglement-enhanced microscope. *Nat. Commun.* **4**, 2426 (2013).
25. Lemos, G. B. et al. Quantum imaging with undetected photons. *Nature* **512**, 409–412 (2014).
26. Kalashnikov, D. A., Paterova, A. V., Kulik, S. P. & Krivitsky, L. A. Infrared spectroscopy with visible light. *Nat. Photon.* **10**, 98–101 (2016).
27. Paterova, A. V., Yang, H., An, C., Kalashnikov, D. A. & Krivitsky, L. A. Tunable optical coherence tomography in the infrared range using visible photons. *Quantum Sci. Technol.* **3**, 025008 (2018).
28. Zhang, L. et al. Spectral tracing of deuterium for imaging glucose metabolism. *Nat. Biomed. Eng.* **3**, 402–413 (2019).
29. Tian, F. et al. Monitoring peripheral nerve degeneration in ALS by label-free stimulated Raman scattering imaging. *Nat. Commun.* **7**, 13283 (2016).
30. Liu, B. et al. Label-free spectroscopic detection of membrane potential using stimulated Raman scattering. *Appl. Phys. Lett.* **106**, 173704 (2015).
31. Konstanze, T. et al. Phenazine production promotes antibiotic tolerance and metabolic heterogeneity in *Pseudomonas aeruginosa* biofilms. *Nat. Commun.* **10**, 762 (2019).
32. Saar, B. G. et al. Video-rate molecular imaging in vivo with stimulated Raman scattering. *Science* **330**, 1368–1370 (2010).
33. Freudiger, C. W. et al. Stimulated Raman scattering microscopy with a robust fibre laser source. *Nat. Photon.* **8**, 153–159 (2014).
34. Freudiger, C. W. et al. Label-free biomedical imaging with high sensitivity by stimulated Raman scattering microscopy. *Science* **322**, 1857–1861 (2008).
35. Pooser, R. C. & Lawrie, B. Plasmonic trace sensing below the photon shot noise limit. *ACS Photon.* **3**, 8–13 (2016).
36. Dowran, M., Kumar, A., Lawrie, B. J., Pooser, R. C. & Marino, A. M. Quantum-enhanced plasmonic sensing. *Optica* **5**, 628–633 (2018).
37. Michael, A. et al. Biological measurement beyond the quantum limit. *Nat. Photon.* **7**, 229–233 (2013).
38. Michael, A. et al. Subdiffraction-limited quantum imaging within a living cell. *Phys. Rev. X* **4**, 011017 (2014).
39. Tenne, R. et al. Super-resolution enhancement by quantum image scanning microscopy. *Nat. Photon.* **13**, 116–122 (2019).
40. Phan, N. M., Cheng, M. F., Bessarab, D. A. & Krivitsky, L. A. Interaction of fixed number of photons with retinal rod cells. *Phys. Rev. Lett.* **112**, 213601 (2014).

41. Choi, Y. et al. Shot-noise-limited two-color stimulated Raman scattering microscopy with a balanced detection scheme. *J. Phys. Chem. B* **124**, 2591–2599 (2020).
42. de Andrade, R. B. et al. Quantum-enhanced continuous-wave stimulated Raman spectroscopy. *Optica* **7**, 470–475 (2020).
43. Triginer Garces, G. et al. Quantum-enhanced stimulated emission detection for label-free microscopy. *Appl. Phys. Lett*. **117**, 024002 (2020).
44. Okuno, M. et al. Quantitative CARS molecular fingerprinting of single living cells with the use of the maximum entropy method. *Angew. Chem*. **122**, 6925–6929 (2010).
45. Kochan, K., Peng, H., Wood, B. R. & Haritos, V. S. Single cell assessment of yeast metabolic engineering for enhanced lipid production using Raman and AFM-IR imaging. *Biotechnol. Biofuels* **11**, 106 (2018).
46. *A Roadmap for Quantum Technologies in the UK* 16 (UK Quantum Technologies Programme, 2015); https://epsrc.ukri.org/newsevents/pubs/quantumtechroadmap
47. Vahlbruch, H., Mehmet, M., Danzmann, K. & Schnabel, R. Detection of 15 dB squeezed states of light and their application for the absolute calibration of photoelectric quantum efficiency. *Phys. Rev. Lett*. **117**, 110801 (2016).
48. Hoover, E. E. & Squier, J. A. Advances in multiphoton microscopy technology. *Nat. Photon*. **7**, 93–101 (2013).
49. Zong, C. et al. Plasmon-enhanced stimulated Raman scattering microscopy with single-molecule detection sensitivity. *Nat. Commun*. **10**, 5318 (2019).
50. Michael, Y., Bello, L., Rosenbluh, M. & Pe'er, A. Squeezing-enhanced Raman spectroscopy. *npj Quantum Inf*. **5**, 81 (2019).

Data availability

The data that support the findings of this study are included in the Supplementary Information. This includes data quantifying the detector design and performance (Supplementary Figs. 3–5); example power spectral densities of the stimulated Raman signal-to-noise ratio with and without squeezing (Supplementary Fig. 6); the raw measured power spectral densities of detector electronic noise, shot-noise and squeezing (Supplementary Fig. 7); experimental measurements of the squeezed variance and classical deamplification of the Stokes field as a function of the optical parametric amplifier pump power (Supplementary Fig. 9); the photocurrent power spectral density used to determine the concentration sensitivity when probing the CH aromatic stretch band in polystyrene (Supplementary Fig. 10); measurements of cell photodamage (Supplementary Fig. 11); and comparative cell images with and without quantum enhancement (Supplementary Fig. 12). Further data are available from the corresponding author upon reasonable request. Source data are provided with this paper.

Acknowledgements We acknowledge W. Wasserman for sourcing the yeast cells in trying circumstances, U. Hoff for contributions to the construction of the apparatus and APE GmbH for support related to the laser system. This work was supported primarily by the Air Force Office of Scientific Research (AFOSR) grant FA2386-14-1-4046. It was also supported by the Australian Research Council Centre of Excellence for Engineered Quantum Systems (EQUS, CE170100009). W.P.B. acknowledges the Australian Research Council Future Fellowship, FT140100650. M.A.T. acknowledges the Australian Research Council Discovery Early Career Research Award, DE190100641.

Author contributions C.A.C., A.T., L.S.M. and M.A.T. collected the data. C.A.C. and A.T. performed the data analysis. C.A.C., A.T. and L.S.M. constructed the experiment. M.W. constructed the microscope, with contributions from M.A.T. and L.S.M. K.B. and B.H. designed and built the photodetector used to observe the stimulated Raman signal. C.A.C., L.S.M., M.A.T. and W.P.B. designed the experiment. M.A.T. and W.P.B. conceived the idea. W.P.B., M.A.T., A.T. and C.A.C. wrote the manuscript with contributions from all authors. W.P.B. led the project with assistance from M.A.T. and L.S.M.

Competing interests The authors declare no competing interests.

Additional information
Supplementary information The online version contains supplementary material available at https://doi.org/10.1038/s41586-021-03528-w.
Correspondence and requests for materials should be addressed to W.P.B.
Peer review information *Nature* thanks the anonymous reviewers for their contribution to the peer review of this work. Peer reviewer reports are available.
Reprints and permissions information is available at http://www.nature.com/reprints.